Journal of Inorganic and General Chemistry
ZAAC
Zeitschrift für anorganische und allgemeine Chemie
DOI: 10.1002/zaac.201800286
ARTICLE

A 2D Zinc Coordination Polymer Built from the Mono-deprotonated 4,4′-Azobis(3,5-dimethyl-1H-pyrazole) Ligand

Simon Millan,[a] Beatriz Gil-Hernández,[b] Emrah Hastürk,[a] Alexa Schmitz,[a] and Christoph Janiak*[a]

Dedicated to Professor Werner Uhl on the Occasion of his 65 Birthday

Abstract. 4,4′-Azobis(3,5-dimethyl-1H-pyrazole) (H_2azbpz) in its mono-deprotonated form as a pyrazole-pyrazolate ligand was assembled together with zinc(II) into the two-dimensional coordination polymer [Zn(Hazbpz)NO_3]·1.25DMF with **sql-a** topology, constituted by the dinuclear $\{Zn_2(\mu\text{-pz})_2(Hpz)_2\}^{2+}$ secondary building unit. The μ_3- bridging mode of the ligand is in analogy to bridging modes observed for 4-(4-pyridyl)pyrazolates ligands. After the removal of the DMF solvent molecules, ethanol can be adsorbed up to a maximum uptake of 276 mg·g^{-1} at p/p_0 = 0.9 in an S-shaped adsorption isotherm, corresponding to two ethanol molecules per [Zn(Hazbpz)NO_3] formula unit. The desorption isotherm reveals that only one EtOH is desorbed until p/p_0 = 0.4 and the other one remains hydrogen-bonded in the framework until very low pressures.

Introduction

Coordination polymers are of interest due to their intriguing topologies and their wide-spreading properties.[1] Structures of one- and two-dimensional coordination polymers have additional weak interactions (e.g. hydrogen bonds, π–π stacking, halogen bonds) besides the polymer-defining coordinative metal–ligand bonds.[2] In this context pyrazole are interesting ligands with a pyridinic and a pyrrolic nitrogen atom next to each other. Pyrazole ligands feature a multifaceted coordination and supramolecular chemistry with interesting catalytic, magnetic, and optical properties.[3] Furthermore, bipyrazole ligands are predestined to construct coordination networks with transition metals as outlined in a recent review by *Pettinari* et al.[4] Bipyrazole ligands can either be used in their non-deprotonated forms as neutral bridging ligands or in their deprotonated forms as anionic bridging ligands. In their neutral forms bipyrazoles build coordination frameworks related to 4,4′-bipyridines with the adjacent N-H functions interacting with hydrogen accepting guest molecules and anions.[5] Their doubly deprotonated forms – the bipyrazolates – build thermally and chemically stable metal-organic frameworks through strong metal-ligand bonds between the metal cation and the pyrazolate anion.

Metal-bipyrazolates show interesting properties like flexibility upon gas adsorption,[6] tunable water sorption properties,[7] or catalytic activity.[8] The simplest bipyrazole representatives 4,4′-bipyrazolyl[5b] and 3,3′,5,5′-tetramethyl-4,4′-bipyrazolyl[5a] are supplemented by bipyrazoles with different spacer groups between the pyrazole rings or substituents on position 3 and 5 of the pyrazole ring in order to obtain a large variety of coordination networks.[7,9] Additionally, bipyrazoles can be used together with carboxylates in the construction of a multitude of coordination networks.[10] On the other hand, the incorporation of mono-deprotonated bipyrazolate, that is, pyrazole-pyrazolate ligands, into coordination compounds is rather scarce. Examples are a dinuclear nickel complex[11] and a ruthenium complex.[12] An early example for a coordination network containing a pyrazole-pyrazolate ligand is an europium MOF, which was synthesized from the metal in the melt of the ligand, containing neutral and mono-anionic 3,3′,5,5′-tetramethyl-4,4′-bipyrazolyl.[13]

Coordination networks built from a pyrazole-pyrazolate and an additional dicarboxylate ligand include a cobalt-coordination polymer containing the mono-deprotonated ligand 4,4′-methylenebis(3,5-dimethyl-1H-pyrazole) and a piperazine-based dicarboxylate[14] and three cobalt(II) or zinc(II) MOFs synthesized from mono-deprotonated 3,3′,5,5′-tetramethyl-4,4′-bipyrazole and 4,4′-biphenyldicarboxylate.[15]

Herein we present [Zn(Hazbpz)NO_3]·1.25DMF as the first coordination polymer with the bipyrazole ligand 4,4′-azobis(3,5-dimethyl-1H-pyrazole) (H_2azbpz) (Scheme 1) and investigated its sorption properties towards water and ethanol.

Results and Discussion

4,4′-Azobis(3,5-dimethyl-1H-pyrazole) (H_2azbpz) was synthesized in four steps starting from acetylacetone (**1**). H_2azbpz was first described by *Hüttel* et al. in 1955 during their studies on nitro- and nitrosopyrazoles via a Mills coupling reaction,

* Prof. Dr. C. Janiak
E-Mail: janiak@uni-duesseldorf.de
[a] Institut für Anorganische Chemie und Strukturchemie
Heinrich-Heine Universität Düsseldorf
40204 Düsseldorf, Germany
[b] Departamento de Química
Facultad de Ciencias de La Laguna, Sección Química
Universidad de La Laguna
38206, La Laguna, Tenerife, Spain
Supporting information for this article is available on the WWW under **http://dx.doi.org/10.1002/zaac.201800286** or from the author.

 © 2018 WILEY-VCH Verlag GmbH & Co. KGaA, Weinheim

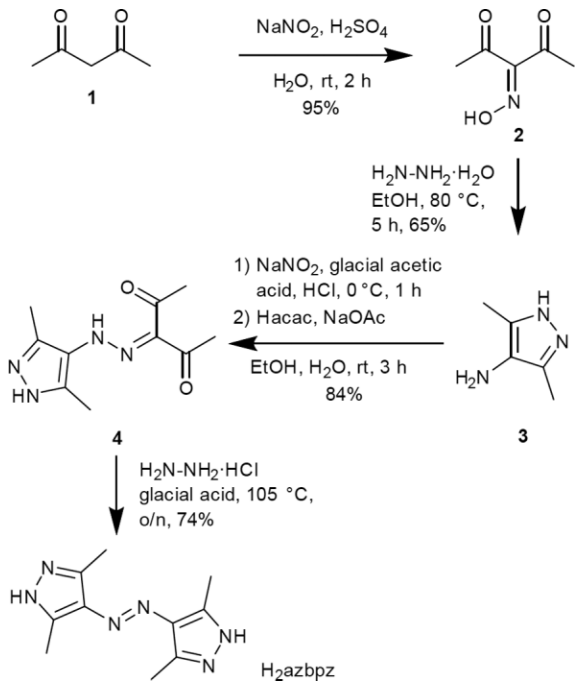

Scheme 1. Reaction scheme for the synthesis of H_2azbpz.

but to the best of our knowledge was never used for the construction of coordination compounds.[16]

A solvothermal reaction between zinc nitrate and H_2azbpz in dimethylformamide (DMF) and ethanol (EtOH) at 80 °C resulted in plate-shaped yellow single crystals. The representative nature of the selected crystals with respect to the bulk was verified by positive matching of the simulated and experimental powder X-ray diffractograms (Figure S1, Supporting Information). The single-crystal X-ray analysis revealed a coordination polymer with formula [Zn(Hazbpz)NO_3]·1.25DMF. The product crystallizes in the monoclinic space group $P2_1/n$ with one zinc(II) ion, one mono-deprotonated ligand Hazbpz$^-$, one nitrate ligand, and 1.25 DMF molecules in the asymmetric unit (Figure 1). The N–H function of the non-deprotonated pyrazole group forms a hydrogen bond to the carbonyl function of one DMF molecule. The other DMF molecule is only a quarter occupied and highly disordered as it sits on a special position (inversion center) of higher symmetry than the DMF molecule itself has (Figure S6, Supporting Information). The solvent content is also underpinned by the thermogravimetric analysis (TGA) and elemental analysis data (Figure 7, Experimental Section).

The zinc(II) ion is tetrahedrally coordinated by three nitrogen atoms and one nitrate oxygen atom. Two nitrogen atoms belong to two bridging pyrazolates (N1 and N2) and the third one belongs to nitrogen N6 from the neutral pyrazole group. Selected bond lengths and angles are given in Table 1. Each mono-deprotonated pyrazole-pyrazolate ligand bridges between three zinc atoms through its non-hydrogen-carrying nitrogen atoms in the heterocycles (Figure 1). Two κN1:κN2-bridging pyrazolates (pz), two coordinated pyrazoles (Hpz), and two terminal nitrato ligands form the inversion-symmetric dinuclear secondary building unit (SBU)

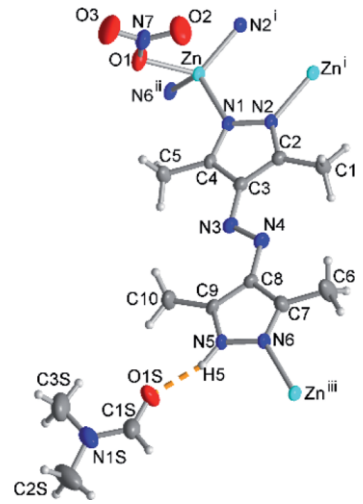

Figure 1. Extended asymmetric unit of [Zn(Hazbpz)NO_3]·1.25DMF (50 % thermal ellipsoids, symmetry transformations: (i) –x, –y+2, –z+1; (ii) x–1/2, –y + 3/2, z + 1/2; (iii) x + 1/2, –y + 3/2, z–1/2.). The disordered DMF molecule is omitted for clarity. Hydrogen bond (dashed orange line) distances /Å and angle /°: N–H 0.92(5), H···O 1.85(5), N···O 2.698(5), D–H···A 153(5).

$\{Zn_2(\mu\text{-pz})_2(Hpz)_2(NO_3)_2\}$ with a Zn···Zn distance of 3.588(8) Å (Figure 2).

Table 1. Selected bond lengths /Å and angles /° in [Zn(Hazbpz)NO_3]·1.25DMF.

Zn–N1	1.969(3)	N1–Zn–O1	112.44(15)
Zn–N2^i	1.977(3)	N2^i–Zn–O1	118.50(15)
Zn–O1	2.020(3)	N1–Zn–N6^{ii}	113.26(14)
Zn–N6^{ii}	2.023(4)	N2^i–Zn–N6^{ii}	106.89(15)
N1–Zn–N2^i	111.78(14)	O1–Zn–N6^{ii}	92.35(14)

Symmetry transformations: (i) –x, –y+2, –z+1; (ii) x–1/2, –y + 3/2, z + 1/2.

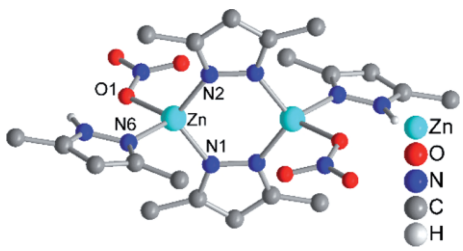

Figure 2. $\{Zn_2(\mu\text{-pz})_2(Hpz)_2(NO_3)_2\}$ as the dinuclear building block (the hydrogen atoms at the methyl groups are omitted for clarity).

The mono-deprotonated Hazbpz$^-$ ligand is perfectly planar and links the square planar 4-c secondary building units to form a two dimensional **sql-a** (= **fes**) net (Figure 3).[17] The dimensions of the rhomboid grid are 12.0×12.0 Å^2 with angles of 70° and 110° measured between the centers of the dinuclear Zn_2 SBU.

 © 2018 WILEY-VCH Verlag GmbH & Co. KGaA, Weinheim

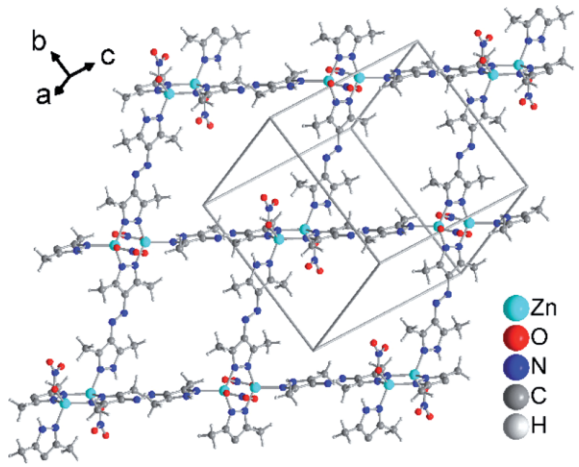

Figure 3. Section of the packing diagram of 2D-[Zn(Hazbpz)NO_3]·1.25DMF with the DMF molecules omitted for clarity.

The square planar 4-c SBU can be topologically represented as a rhomboid building block linked by the azo-functionalities (Figure 4). The [Zn(Hazbpz)NO_3] layers stack in an AB fashion with a symmetry relation of [x+1, *y*, *z*] or [x, *y*, *z* + 1] between the nets and the dinuclear "Zn_2"-SBUs of the adjacent grids sitting in the middle of the openings (Figure 5 and Figure 6). No significant supramolecular interactions could be identified between the layers.

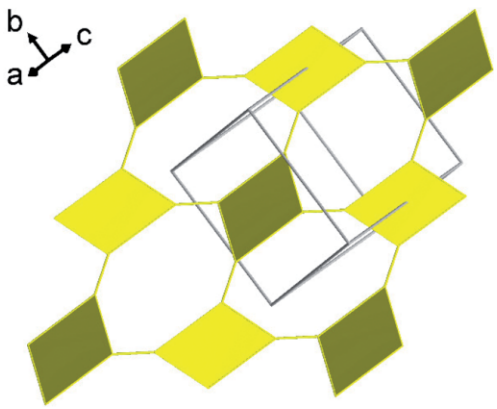

Figure 4. Topological **sql-a** representation of a single [Zn(Hazbpz)NO_3] layer with the $\{Zn_2(\mu\text{-pz})_2(Hpz)_2(NO_3)_2\}$-SBU as yellow rhomboids linked by the azo-functionalities.

Analogous dinuclear metal units $\{M_2(\mu\text{-pz})_2(Hpz)_2\}^{2+}$ can be found with *M* = Zn and Co.[18] *Pettinari* et al. noted that with an excess of 1H-pyrazole, the compound $[Zn(\mu\text{-pz})(Hpz)(CH_3COO)]_2$, built from the aforementioned dinuclear units, is formed. The dinuclear molecules transform with thermal treatment into the polymeric $[Zn(\mu\text{-pz})_2]$-form. This transformation was not observed for the 3,5-dimethylpyrazole analog.[18b] *Baruah* et al. found that the utilization of DMF favored the formation of the dinuclear pyrazolato-bridged complexes in contrast to monomeric pyrazole complexes in reactions of zinc acetate, 1H-3,5-dimethylpyrazole and aromatic carboxylic acids.[18c] Besides the cobalt coordination polymer by *Batten* et al., built from the mono-

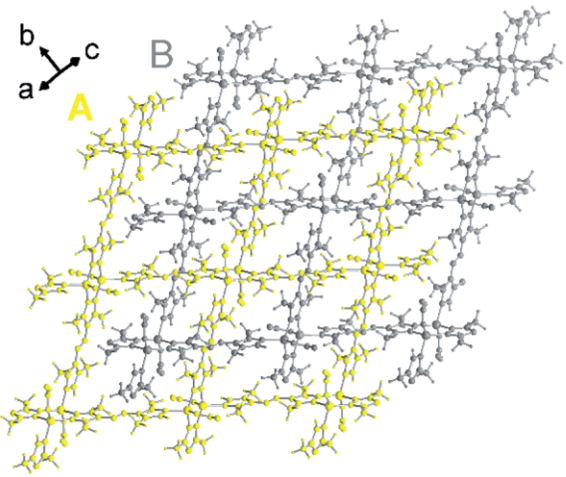

Figure 5. Section of the packing diagram of two adjacent two-dimensional nets of [Zn(Hazbpz)NO_3]·1.25DMF. DMF molecules are omitted for clarity; symmetry relation between layer A (yellow) and layer B (grey): *x* + 1, *y*, *z* or x, *y*, *z* + 1.

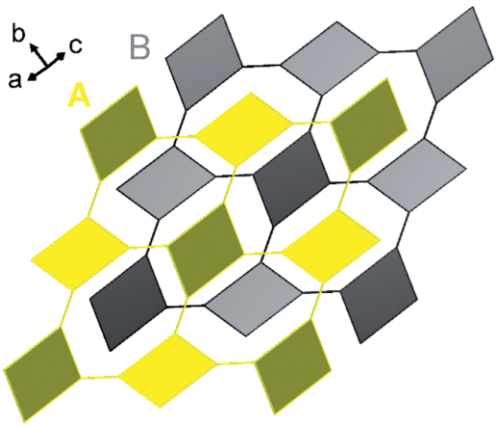

Figure 6. Topological **sql-a** representation of two adjacent AB-stacked 2D layers.

deprotonated ligand 4,4′-methylenebis(3,5-dimethyl-1H-pyrazole) and 1,4-bis((3-carboxyphenyl)methyl)piperazine (Figure S7, Supporting Information),[14] our compound [Zn(Hazbpz)NO_3]·1.25DMF is, to the best of our knowledge, the only coordination polymer assembled from the $\{M_2(\mu\text{-pz})_2(Hpz)_2\}^{2+}$ entity (Figures S8–S10, Supporting Information).

It is interesting to note the similarities of the coordination behavior of the mono-deprotonated ligand $Hazbpz^-$ and 4-(4-pyridyl)pyrazolates (Hpypz) (Figure S5, Supporting Information). The latter are an extension of the intensively studied 1,2,4-triazolate system.[19] *Turner* et al. have synthesized the directly related framework $[Zn_2(pypz)_2Cl_2]$·2EtOH,[20] which is identical in its topology to [Zn(Hazbpz)NO_3]·1.25DMF. *Chen* et al. used these cationic $[Zn(pypz)]^+$ **sql-a** sheets with $[Zn_2(btc)_4(H_2O)_2]^{8-}$ pillars to obtain a three-dimensional porous MOF with a high methane storage capacity.[21]

The TGA data of [Zn(Hazbpz)NO_3]·1.25DMF as-synthesized (a.s) show a two-step weight loss up to 200 °C, which

 © 2018 WILEY-VCH Verlag GmbH & Co. KGaA, Weinheim

corresponds to a total weight loss of 19.9 % (Figure 7). The first step of 4.0 % in the range of 100–150 °C is assigned to the disordered and not hydrogen-bonded quarter-occupied DMF molecule (4.2 % theoretically) and the second step with 15.9 % in the range of 150–210 °C to the hydrogen-bonded DMF molecule (16.1 % theoretically). After the sample was degassed at 150 °C for 12 h under vacuum (10^{-5} mbar) the TGA curve of the activated sample shows that the solvent molecules had been fully removed (Figure 5). Solvent-depleted [Zn(Hazbpz)NO_3] is thermally stable up to 340 °C.

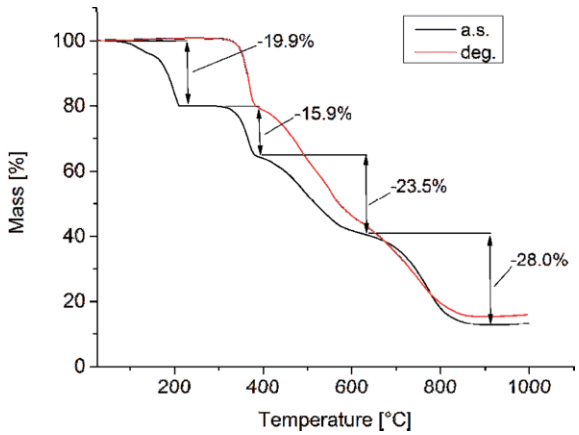

Figure 7. TGA curve of [Zn(Hazbpz)NO_3]·1.25DMF as-synthesized (a.s.) and degassed (deg.) with a heating rate of 5 K·min^{-1} in a N_2 atmosphere.

Since the included solvent molecules could be removed, the sorption properties of degassed (deg.) [Zn(Hazbpz)NO_3] towards H_2O and EtOH vapors were tested (Figure 8). [Zn(Hazbpz)NO_3]-(deg.) adsorbs about 51 mg·g^{-1} H_2O at p/p_0 = 0.9, which equals about one H_2O molecule per [Zn(Hazbpz)NO_3] formula unit. For ethanol [Zn(Hazbpz)NO_3]-(deg.) shows an S-shaped adsorption isotherm with the main step between 0.5 and 0.7 p/p_0 and a maximum uptake of 276 mg·g^{-1} at p/p_0 = 0.9, representing about two EtOH molecules per formula unit. The desorption curve

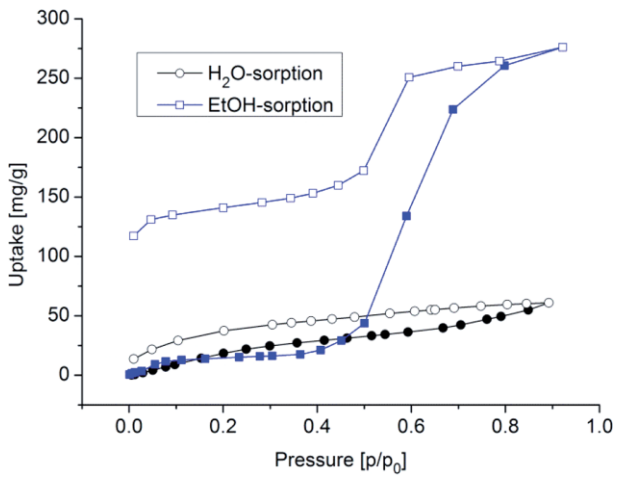

Figure 8. Water (black) and ethanol (blue) sorption isotherms at 293 K for [Zn(Hazbpz)NO_3]-(deg.).

shows a large hysteresis with a very slow desorption below p/p_0 = 0.4 or around 140 mg·g^{-1}, where about one EtOH molecule per [Zn(Hazbpz)NO_3] formula unit would be present. This means that only one EtOH is desorbed until p/p_0 = 0.4 and the other one remains hydrogen-bonded in the framework until very low pressures. Under the chosen measurement times, the desorption curve did not close. The last desorption data point at p/p_0 = 0.01 indicates the beginning desorption of the second hydrogen-bonded ethanol molecule.

Conclusions

The novel two-dimensional coordination polymer [Zn(Hazbpz)NO_3]·1.25DMF with **sql-a** topology was structurally characterized. The compound is based on the bipyrazole ligand H_2azbpz, which was until now not used in the construction of coordination networks. The vapor sorption characteristics for water and ethanol with the S-shaped adsorption isotherm of ethanol and a pronounced hysteresis confirm the hydrophobic nature of the material. In its mono-deprotonated version Hazbpz$^-$ is a pyrazole-pyrazolate ligand and mimics the coordination behavior of 1,2,4-triazolates and 4-(4-pyridyl)pyrazolates. We hypothesize that by careful adjustment of the synthesis conditions this coordination behavior of bipyrazoles with a N–H hydrogen-bond donor function directly adjacent to the metal subunits can be very useful in the construction of a wide set of novel coordination polymers.

Experimental Section

The chemicals used were obtained from commercial sources. No further purification was carried out. CHN analysis was performed with a Perkin–Elmer CHN 2400 (Perkin–Elmer, Waltham, MA, USA). IR spectra were recorded with a Bruker Tensor 37 IR spectrometer (Bruker Optics, Ettlingen, Germany) with a KBr unit. ^1H and ^{13}C spectra were measured with a Bruker Advance DRX-300. ESI-MS spectra were recorded with a Thermo Quest Ion Trap API mass spectrometer Finnigan LCQ Deca. Thermogravimetric analysis (TGA) was done with a Netzsch TG 209 F3 Tarsus (Netzsch, Selb, Germany) in the range from 25 to 1000 °C, equipped with an Al_2O_3-crucible and applying a heating rate of 5 K·min^{-1} in a nitrogen atmosphere. The powder X-ray diffraction pattern (PXRD) was obtained with a Bruker D2 Phaser powder diffractometer with a flat silicon, low background sample holder, at 30 kV, 10 mA for Cu-K_α radiation (λ = 1.5418 Å). The water and ethanol sorption isotherms were measured at 293 K using a Quantachrome VSTAR vapor sorption analyzer. The sample was activated with a Quantachrome FloVac Degasser at 150 °C for 12 h under a vacuum of 10^{-5} mbar.

Single Crystal X-ray Structure: Suitable crystals were carefully selected under a polarizing microscope, covered in protective oil and mounted on a 0.05 mm cryo loop. Data collection: Bruker Kappa APEX2 CCD X-ray diffractometer (Bruker AXS Inc., Madison, WI, USA) with microfocus tube, Mo-K_α radiation (λ = 0.71073 Å), multilayer mirror system, ω-scans; data collection with APEX2,[22] cell refinement with SMART and data reduction with SAINT,[22] experimental absorption correction with SADABS.[23] Structure analysis and refinement: The structure was solved by direct methods using SHELXL2016,[24] refinement was done by full-matrix least-squares on F^2 using the SHELX-97 program suite. Crystal data and details on

 © 2018 WILEY-VCH Verlag GmbH & Co. KGaA, Weinheim

the structure refinement are given in Table 2. Graphics were drawn with Diamond.[25]

Table 2. Crystal structure and refinement details of [Zn(Hazbpz)NO_3]·1.25DMF.

	[Zn(Hazbpz)NO_3]·1.25DMF
Empirical formula	[$C_{10}H_{13}N_7O_3Zn$]·1.25(C_3H_7NO)
M_r /g·mol^{-1}	436.01
Crystal system	monoclinic
Space group	$P2_1/n$
Crystal size /mm	0.05 × 0.05 × 0.01
Temperature /K	150
a /Å	10.7845 (12)
b /Å	13.7644 (14)
c /Å	13.8068 (14)
β /°	104.715 (6)
V /Å^3	1982.3 (4)
Z	4
μ /mm^{-1}	1.28
F(000)	904
Max./min. transmission	0.750/0.680
Measured, indep., observed reflections	21901, 2993, 2337 [$I > 2\sigma(I)$]
R_{int}	0.053
Data / restraints / parameters	2993 / 1 / 256
Max./min. $\Delta\rho$ [a] /e·Å^{-3}	0.834, –0.370
R, $wR(F^2)$, S [$I > 2\sigma$ (I)] [b]	0.0433, 0.1173, 1.086
R, $wR(F^2)$, S [all data] [b]	0.0614, 0.1261, 1.092

a) Largest difference peak and hole. b) $R_1 = [\Sigma(|F_o| - |F_c|)/\Sigma|F_o|]$; $wR_2 = [\Sigma [w(F_o^2–F_c^2)^2]/\Sigma[w(F_o^2)^2]]^{1/2}$. Goodness-of-fit $S = [\Sigma [w(F_o^2–F_c^2)^2] /(n–p)]^{1/2}$.

Crystallographic data (excluding structure factors) for the structure in this paper have been deposited with the Cambridge Crystallographic Data Centre, CCDC, 12 Union Road, Cambridge CB21EZ, UK. Copies of the data can be obtained free of charge on quoting the depository number CCDC-1852726 (Fax: +44-1223-336-033; E-Mail: deposit@ccdc.cam.ac.uk, http://www.ccdc.cam.ac.uk).

2,3,4-Pentanetrione-3-oxime (**2**) was prepared according to *Tkach* et al. and used without purification.[26] Subsequently, 4-amino-3,5-dimethyl-1H-pyrazole (**3**) was synthesized through a procedure adapted from *Liu* et al.[27] and coupled in a Japp-Klingemann reaction to obtain 3-(2-(3,5-dimethyl-1H-pyrazolyl)hydrazone)pentan-2,4-dione (**4**) according to *Rollas* et al.[28]

4,4′-Azobis(3,5-dimethyl-1H-pyrazole) (H_2azbpz): 3-(2-(3,5-Dimethyl-1H-pyrazolyl)hydrazone)pentan-2,4-dione (2.01 g, 9.05 mmol) and hydrazine monohydrochloride (0.740 g, 10.8 mmol, 1.2 equiv.) dissolved in 15 mL of glacial acetic acid were heated at 105 °C overnight. The yellow precipitate was filtered off and washed thoroughly with water. The crude product was recrystallized from an ethanol:water mixture to afford H_2azbpz as a yellow powder. After drying for 48 h at 60 °C in a vacuum oven (10^{-1} mbar) 1.47 g (6.73 mmol, 74 %) were obtained. **^{1}H NMR** (300 MHz, [D_6]DMSO): δ = 2.37, 12.36. **^{13}C NMR** (75 MHz), [D_6]DMSO): δ = 141.45, 135.49, 134.39, 13.64, 9.97 ppm. **ESI-MS**: $[M + H]^+$ 219.3. Calcd. for H_2azbpz. $C_{10}H_{15}N_6$: calcd. C 55.03, H 6.47, N 38.50 %; found: C 54.89, H 6.49 N 38.24 %.

[Zn(Hazbpz)NO_3]·1.25DMF: H_2azbpz (18 mg, 0.083 mmol) dissolved in 2 mL of EtOH and 0.3 mL of DMF were combined with a solution of $Zn(NO_3)_2$·$4H_2O$ (10 mg, 0.038 mmol) in 1 mL of EtOH and put in a preheated oven at 80 °C for 4 d. Yield: 3.4 mg (21 %). In a scaled-up synthesis H_2azbpz (108.1 mg, 0.50 mmol) was dissolved in 15 mL of EtOH and 1.8 mL of DMF and combined with $Zn(NO_3)_2$·$4H_2O$ (60.2 mg, 0.23 mmol) dissolved in 3 mL of EtOH in a 50 mL Pyrex vessel. After 4 d at 80 °C in an isothermal oven, the product was thoroughly washed with a 10 v/v% DMF/EtOH mixture. [Zn(Hazbpz)NO_3]·1.25DMF was obtained by suction filtration and short drying in air. Yield: 76.0 mg (75 %). [Zn(Hazbpz)NO_3]·1.25DMF, $C_{13.75}H_{21.75}N_{8.25}O_{4.25}Zn$: calcd. C 37.88, H 5.03, N 26.50 %; found: C 38.06, H 5.11, N 25.58 %. [Zn(Hazbpz)NO_3]-(degassed), $C_{10}H_{13}N_7O_3Zn$: calcd. C 34.85, H 3.80, N 28.45 %; found: C 34.97, H 3.86, N 27.78 %.

Supporting Information (see footnote on the first page of this article): PXRD patterns; NMR, IR spectra; SBUs of mono-deprotonated bipyrazoles with dicarboxylates from the literature; symmetry transformation between two adjacent nets.

Acknowledgements

The work was supported by the Federal German Ministry of Education and Research (BMBF) under grant-# 03SF0492C (Optimat).

Keywords: Coordination polymer; Bipyrazole; Zinc; Pyrazole-pyrazolate; Ethanol sorption; Hysteresis

References

[1] a) S. R. Batten, R. Robson, *Angew. Chem. Int. Ed.* **1998**, *37*, 1460–1494; b) C. Janiak, *Dalton Trans.* **2003**, 2781–2804; c) S. Kitagawa, R. Kitaura, S.-i. Noro, *Angew. Chem. Int. Ed.* **2004**, *43*, 2334–2375; d) L. Carlucci, G. Ciani, D. M. Proserpio, *Coord. Chem. Rev.* **2003**, *246*, 247–289; e) N. Li, R. Feng, J. Zhu, Z. Chang, X.-H. Bu, *Coord. Chem. Rev.* **2018** , in press; DOI: 10.1016/j.ccr.2018.05.016.

[2] a) C. B. Aakeröy, N. R. Champness, C. Janiak, *CrystEngComm* **2010**, *12*, 22–43; b) K. Uemura, K. Saito, S. Kitagawa, H. Kita, *J. Am. Chem. Soc.* **2006**, *128*, 16122–16130; c) B. Paul, B. Zimmermann, K. M. Fromm, C. Janiak, *Z. Anorg. Allg. Chem.* **2004**, *630*, 1650–1654; d) B. Wisser, Y. Lu, C. Janiak, *Z. Anorg. Allg. Chem.* **2007**, *633*, 1189–1192; e) S. Sengupta, S. Ganguly, A. Goswami, P. K. Sukul, R. Mondal, *CrystEngComm* **2013**, *15*, 8353–8365; f) B. Gil-Hernandez, H. A. Höppe, J. K. Vieth, J. Sanchiz, C. Janiak, *Chem. Commun.* **2010**, *46*, 8270–8272; g) Y. Yong, Z. Ning-Ning, L. Rong, X. Jian-Gang, L. Jian, Z. Fa-Kun, G. Guo-Cong, *Eur. J. Inorg. Chem.* **2017**, *2017*, 3811–3814; h) S. Millan, G. Makhloufi, C. Janiak, *Crystals* **2018**, *8*, 30; i) A. Azhdari Tehrani, S. Abedi, A. Morsali, *Cryst. Growth Des.* **2017**, *17*, 255–261; j) B. L. Martinez, R. L. LaDuca, *Z. Anorg. Allg. Chem.* **2017**, *643*, 1118–1125.

[3] a) S. Trofimenko, *Chem. Rev.* **1972**, *72*, 497–509; b) A. P. Sadimenko, S. S. Basson, *Coord. Chem. Rev.* **1996**, *147*, 247–297; c) M. A. Halcrow, *Dalton Trans.* **2009**, 2059–2073; d) M. Viciano-Chumillas, S. Tanase, L. J. de Jongh, J. Reedijk, *Eur. J. Inorg. Chem.* **2010**, *2010*, 3403–3418; e) C. W. Lu, Y. Wang, Y. Chi, *Chem. Eur. J.* **2016**, *22*, 17892–17908.

[4] C. Pettinari, A. Tăbăcaru, S. Galli, *Coord. Chem. Rev.* **2016**, *307*, 1–31.

[5] a) I. Boldog, E. B. Rusanov, A. N. Chernega, J. Sieler, K. V. Domasevitch, *Polyhedron* **2001**, *20*, 887–897; b) I. Boldog, J. Sieler, A. N. Chernega, K. V. Domasevitch, *Inorg. Chim. Acta* **2002**, *338*, 69–77; c) E. B. Rusanov, V. V. Ponomarova, V. V. Komarchuk, H. Stoeckli-Evans, E. Fernandez-Ibañez, F. Stoeckli, J. Sieler, K. V. Domasevitch, *Angew. Chem. Int. Ed.* **2003**, *42*, 2499–2501; d) K. V. Domasevitch, I. Boldog, E. B. Rusanov, J. Hunger, S. Blaurock, M. Schröder, J. Sieler, *Z. Anorg. Allg. Chem.* **2005**, *631*, 1095–1100.

 © 2018 WILEY-VCH Verlag GmbH & Co. KGaA, Weinheim

[6] a) J. A. Mason, J. Oktawiec, M. K. Taylor, M. R. Hudson, J. Rodriguez, J. E. Bachman, M. I. Gonzalez, A. Cervellino, A. Guagliardi, C. M. Brown, P. L. Llewellyn, N. Masciocchi, J. R. Long, *Nature* **2015**, *527*, 357–361; b) H. J. Choi, M. Dincă, J. R. Long, *J. Am. Chem. Soc.* **2008**, *130*, 7848–7850.
[7] C. R. Wade, T. Corrales-Sanchez, T. C. Narayan, M. Dincă, *Energy Environ. Sci.* **2013**, *6*, 2172–2177.
[8] a) Y. Lu, M. Tonigold, B. Bredenkötter, D. Volkmer, J. Hitzbleck, G. Langstein, *Z. Anorg. Allg. Chem.* **2008**, *634*, 2411–2417; b) M. Tonigold, Y. Lu, A. Mavrandonakis, A. Puls, R. Staudt, J. Möllmer, J. Sauer, D. Volkmer, *Chem. Eur. J.* **2011**, *17*, 8671–8695.
[9] a) A. Tăbăcaru, C. Pettinari, N. Masciocchi, S. Galli, F. Marchetti, M. Angjellari, *Inorg. Chem.* **2011**, *50*, 11506–11513; b) E. Q. Procopio, N. M. Padial, N. Masciocchi, S. Galli, J. E. Oltra, E. Barea, J. A. R. Navarro, *CrystEngComm* **2013**, *15*, 9352–9355; c) M. Grzywa, D. Denysenko, A. Schaller, A. Kalytta-Mewes, D. Volkmer, *CrystEngComm* **2016**, *18*, 7883–7893; d) J. Fritzsche, M. Grzywa, D. Denysenko, V. Bon, I. Senkovska, S. Kaskel, D. Volkmer, *Dalton Trans.* **2017**, *46*, 6745–6755.
[10] a) L. Hou, Y.-Y. Lin, X.-M. Chen, *Inorg. Chem.* **2008**, *47*, 1346–1351; b) R. Mondal, M. K. Bhunia, K. Dhara, *CrystEngComm* **2008**, *10*, 1167–1174; c) A. Goswami, S. Sengupta, R. Mondal, *CrystEngComm* **2012**, *14*, 561–572; d) Y.-Q. Sun, S. Deng, Q. Liu, S.-Z. Ge, Y.-P. Chen, *Dalton Trans.* **2013**, *42*, 10503–10509; e) Y.-Q. Sun, S. Deng, S.-Z. Ge, Q. Liu, Y.-P. Chen, *J. Cluster Sci.* **2013**, *24*, 605–617; f) K. Tomar, R. Rajak, S. Sanda, S. Konar, *Cryst. Growth Des.* **2015**, *15*, 2732–2741; g) L.-L. Han, T.-P. Hu, K. Mei, Z.-M. Guo, C. Yin, Y.-X. Wang, J. Zheng, X.-P. Wang, D. Sun, *Dalton Trans.* **2015**, *44*, 6052–6061.
[11] V. Lozan, P. Y. Solntsev, G. Leibeling, K. V. Domasevitch, B. Kersting, *Eur. J. Inorg. Chem.* **2007**, *2007*, 3217–3226.
[12] T. Jozak, D. Zabel, A. Schubert, Y. Sun, W. R. Thiel, *Eur. J. Inorg. Chem.* **2010**, *2010*, 5135–5145.
[13] A. Zurawski, J. Sieler, K. Müller-Buschbaum, *Z. Anorg. Allg. Chem.* **2009**, *635*, 2034–2038.
[14] C. S. Hawes, B. Moubaraki, K. S. Murray, P. E. Kruger, D. R. Turner, S. R. Batten, *Cryst. Growth Des.* **2014**, *14*, 5749–5760.
[15] a) L. Hou, L.-N. Jia, W.-J. Shi, L.-Y. Du, J. Li, Y.-Y. Wang, Q.-Z. Shi, *Dalton Trans.* **2013**, *42*, 6306–6309; b) T. Li, F.-L. Wang, S.-T. Wu, X.-H. Huang, S.-M. Chen, C.-C. Huang, *Cryst. Growth Des.* **2013**, *13*, 3271–3274; c) H.-H. Wang, L.-N. Jia, L. Hou, W.-j. Shi, Z. Zhu, Y.-Y. Wang, *Inorg. Chem.* **2015**, *54*, 1841–1846.
[16] R. Hüttel, F. Büchele, P. Jochum, *Chem. Ber.* **1955**, *88*, 1577–1585.
[17] O. Delgado-Friedrichs, M. O'Keeffe, O. M. Yaghi, *Phys. Chem. Chem. Phys.* **2007**, *9*, 1035–1043.
[18] a) M. K. Ehlert, S. J. Rettig, A. Storr, R. C. Thompson, J. Trotter, *Can. J. Chem.* **1993**, *71*, 1425–1436; b) A. Cingolani, S. Galli, N. Masciocchi, L. Pandolfo, C. Pettinari, A. Sironi, *Dalton Trans.* **2006**, 2479–2486; c) R. Sarma, D. Kalita, J. B. Baruah, *Dalton Trans.* **2009**, 7428–7436; d) U. P. Singh, P. Tyagi, S. Pal, *Inorg. Chim. Acta* **2009**, *362*, 4403–4408; e) S. Jin, D. Wang, *Z. Anorg. Allg. Chem.* **2011**, *637*, 618–625; f) J. Pan, J. Ju, Q. Wei, B. Liu, S. Jin, Z. Lin, D. Wang, *Z. Anorg. Allg. Chem.* **2014**, *640*, 1745–1753.
[19] a) J.-P. Zhang, X.-M. Chen, *Chem. Commun.* **2006**, 1689–1699; b) E.-C. Yang, T.-Y. Liu, Q. Wang, X.-J. Zhao, *Inorg. Chem. Commun.* **2011**, *14*, 285–287; c) K.-J. Chen, R.-B. Lin, P.-Q. Liao, C.-T. He, J.-B. Lin, W. Xue, Y.-B. Zhang, J.-P. Zhang, X.-M. Chen, *Cryst. Growth Des.* **2013**, *13*, 2118–2123; d) Q.-G. Zhai, N. Bai, S. n. Li, X. Bu, P. Feng, *Inorg. Chem.* **2015**, *54*, 9862–9868.
[20] Y. Mulyana, C. J. Kepert, L. F. Lindoy, A. Parkin, P. Turner, *Dalton Trans.* **2005**, 1598–1601.
[21] J.-M. Lin, C.-T. He, P.-Q. Liao, D.-D. Zhou, J.-P. Zhang, X.-M. Chen, *Sci. China: Chem.* **2016**, *59*, 970–974.
[22] *APEX2*, *SAINT*, Data Reduction and Frame Integration Program for the CCD Area-Detector System, Bruker Analytical X-ray Systems; Data Collection Program for the CCD Area-Detector System: Madison, WI, USA, **1997–2006**.
[23] G. Sheldrick, Program for Empirical Absorption Correction of Area Detector Data, University of Göttingen, Germany **1996**.
[24] a) G. M. Sheldrick, *Acta Crystallogr., Sect. C* **2015**, *71*, 3–8; b) G. Sheldrick, *Acta Crystallogr., Sect. A* **2008**, *64*, 112–122.
[25] K. Brandenburg, *DIAMOND*, version 4.5; Crystal and Molecular Structure Visualization; Crystal Impact - K. Brandenburg & H. Putz Gbr., Bonn, Germany, **2009–2018**.
[26] P. A. Nikitina, L. G. Kuz′mina, V. P. Perevalov, I. I. Tkach, *Tetrahedron* **2013**, *69*, 3249–3256.
[27] J. Li, J. Gao, H. Li, X. Yang, Y. Liu, *Anal. Methods* **2014**, *6*, 4305–4311.
[28] B. Koçyiğit Kaymakçıoğlu, S. Rollas, *Farmaco* **2002**, *57*, 595–599.

Received: July 1, 2018
Published online: August 22, 2018

 © 2018 WILEY-VCH Verlag GmbH & Co. KGaA, Weinheim